

# Local Diversity and Ultra-Reliable Antenna Arrays

Jens Abraham and Torbjörn Ekman

**Abstract**—Ultra-reliable low-latency communication enables new use cases for mobile radio networks. The ultra-reliability (UR) regime covers outage probabilities between  $10^{-9}$  and  $10^{-5}$ , obtained under stringent latency requirements. Characterisation of the UR-relevant statistics is difficult due to the rare nature of outage events, but diversity defines the asymptotic behaviour of the small-scale fading distributions' lower tail. The UR-relevant regime in large-scale antenna systems behaves differently from the tail. The generalising *local diversity* at a certain outage probability shows this difference clearly. For more than four independent antenna elements, the classic diversity overestimates and underestimates the slope of the cumulative density function for weak and strong deterministic channel components, respectively.

**Index Terms**—channel hardening, massive MIMO, Rician fading, URLLC.

## I. INTRODUCTION

One of the reoccurring promises in both fifth generation mobile networks (5G) and sixth generation mobile networks (6G) specifications is ultra-reliable low-latency communication (URLLC). The URLLC requires an outage probability of  $10^{-5}$  or better within a 1 ms transmission period in 5G [1]. The authors of [2] introduce the terminology of *ultra-reliability (UR)-relevant statistics* for outage probabilities below  $10^{-5}$ . It can be expected that the requirements for 6G will be even more stringent and we will consider outage probabilities between  $10^{-9}$  and  $10^{-5}$  as the UR-relevant regime.

Generally, the allowed latency can be used to retransmit a packet if the original message did not reach its destination. By decreasing the permitted latency, only one-shot transmissions can ultimately fulfil the requirement because a retransmission will exceed the stringent limit on delay. A potential acknowledgement can inform the user if the packet has been received successfully, to allow for different behaviours in the case of failure.

Overall, link-loss due to small-scale fading can be counteracted with forward error correction (FEC), relying on the assumption that fading events are short enough with respect to the coded packet length. Hence, small scale fading has to be characterised to properly design the FEC.

Massive multiple input multiple output (MIMO) is a technology that improves the link robustness by exploitation of channel hardening. This means simply a diminishing variation of the channel gain around its mean due to antenna diversity. We have recently suggested to use a fading margin to characterise channel hardening [3]. It describes the required excess gain to provide a certain outage probability at a chosen

rate. This allows to clearly quantify the performance of an UR antenna array with varying number of antenna elements.

A subset of use cases for URLLC requires high energy efficiency in addition. In those cases, minimising the fading margin improves the energy efficiency and allows to meet UR target outage probabilities. Furthermore, smaller fading margins reduce the interference levels for users of the same system and systems that share the same spectrum resource. This highlights, why large antenna arrays are a technically viable solution for narrow-band URLLC without retransmission of packets. System level simulations based on a 3GPP channel model for a specific cell show promising results for a coherence interval based pilot strategy [4] to achieve URLLC.

A fundamental question remains, how can we infer the system behaviour of events that barely ever happen? A neat approach is the characterisation of the lower tail of the cumulative distribution function (CDF) as an intermediate solution between parametric channel models and non-parametric models [5]. The lower tail of multiple common fading distributions follows a power law [2], which gives the possibility to relax the model assumption from a single distribution to a class of distributions. The power law approximation requires two parameters: an offset and a log-log slope of the CDF. E.g. the classic Rayleigh channel shows a well known slope of 10 dB per decade in the lower tail.

Furthermore, the outage probability in detection problems [6] for high signal to noise ratio (SNR) corresponds to the lower tail of the channel gain, emphasising the variation introduced due to the small-scale fading channel, avoiding to specify the used modulation and detector. Due to that correspondence, the log-log slope in the asymptotic lower tail reveals the diversity of the radio channel. Evaluating the log-log slope at specific probability gives the generalising *local diversity*. Hence, it attains the classic diversity measure for probabilities converging to zero.

Unfortunately, the slope of the channel gain after multi-antenna combining in both Rayleigh and Rician fading, deviates from the diversity. We will show that a power law approximation can not provide an accurate description of the CDF in the UR-relevant region.

As an alternative, a non-parametric model could be employed to cover the behaviour of rare events that barely ever happen. This would require the least assumptions, but the amount of simulations or measurements needed to get a reliable estimate of the CDF of the effective channel gain in the UR-relevant region is very large (see section II). Especially in dynamic scenarios, the channel non-stationarity restricts the possibility of collecting enough samples for a reliable system prediction even if acquisition of perfect channel state

J. Abraham and T. Ekman are with the Department of Electronic Systems, Norwegian University of Science and Technology, Norway. e-mail: {jens.abraham, torbjorn.ekman}@ntnu.no

information is assumed. This restricts the practical usefulness of a pure non-parametric model.

In section III, the *local diversity* measure is introduced to relate the classical diversity to the probability region of interest. This measure can be seen as the relative error of a power law approximation based on the asymptotic behaviour of the lower tail. An uncorrelated Rician multi-antenna fading environment is introduced in section IV with new compact expressions for the CDF, probability density function (PDF) and local diversity in terms of the complementary Marcum-Q function. This allows to easily evaluate them even for large scale antenna systems. Correlation could be introduced into the mathematical framework, but would require Monte Carlo evaluation to produce results and has been left out for the time being. We provide a comparison of multi-antenna systems in different Rician fading environments with respect to the fading margin in section V, to discuss the scaling behaviour. Furthermore, sampling strategies to analyse the UR-relevant regime are outlined.

## II. PREDICTING THE UNPREDICTABLE?

The reliable estimation of the UR-relevant statistics of any random variable without prior knowledge, requires a lot of observations. The Dvoretzky-Kiefer-Wolfowitz (DKW) inequality [7], [8] can be used to bound an  $n$ -sample empirical cumulative distribution function (ECDF) with respect to the true underlying CDF. The error term  $\epsilon$  with confidence  $\alpha$  is:

$$\epsilon = \sqrt{\frac{\ln \frac{2}{1-\alpha}}{2n}}. \quad (1)$$

This error term is resulting in an error floor for the ECDF at low probabilities. Taking  $n = 10^6$  observations as example and aiming at a confidence of  $\alpha = 99\%$  gives an error term of  $1.6 \times 10^{-3}$ . The resulting upper bound of the ECDF for a true single-antenna Rayleigh fading channel is shown in Fig. 1. It can be seen that the ECDF in the UR-relevant regime would be much smaller than the error floor, rendering empirical estimation of outage probabilities below  $1.6 \times 10^{-3}$  practically useless.

The collection of many realisations from measurements is limited by the channel stationarity, such that each sample belongs to a single CDF. With antenna arrays, spatial sampling is added to spectral and temporal sampling. Especially in high (environmental) mobility scenarios, the temporal stationarity domain is restricted, making estimation of UR-relevant statistics in the lower tail prone to large estimation errors. Additionally, if energy efficient users are required, less spectrum may be used, reducing the number of samples in the spectral domain. Hence, the spatial domain sampling provided by an antenna array has to provide both the robustness of the system as well as the dimension to estimate the CDF. Furthermore, even Monte Carlo simulations become cumbersome for simulating reliable results, because the generation of many samples is time consuming and a subset of the results needs to be kept in memory for the ECDF. Analytic study has the possibility to

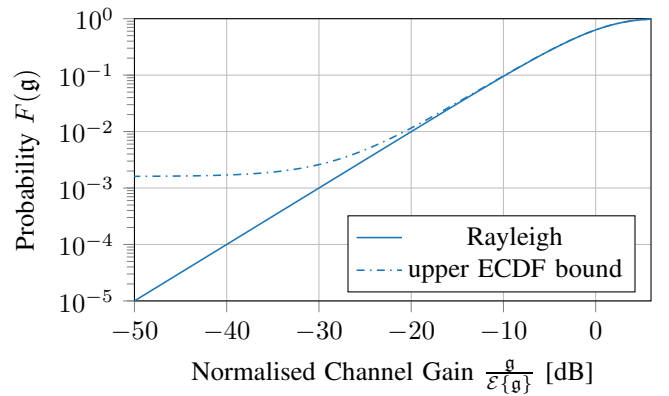


Fig. 1. The CDF of a Rayleigh fading channel and an upper bound for an ECDF is shown. The error term in Eqn. (1) for a million observations and a confidence interval of 99% is used as example, making estimation of outage probabilities below  $1.6 \times 10^{-3}$  unreliable.

give insight into the UR-relevant region, as long as the model assumptions are not violated.

## III. LOCAL DIVERSITY

We define the *local diversity* as the derivative of the scaled logarithmic CDF of the channel gain  $g$  in dB:

$$D(g) = \frac{\partial}{\partial 10g/10} 10 \log_{10}(F(g)) = g \frac{f(g)}{F(g)}. \quad (2)$$

Solving the differentiation reveals the quotient between PDF  $f(g)$  and CDF  $F(g)$ , also known as inverse Mills' ratio, multiplied with  $g$ . The scaling ensures that a Rayleigh fading channel provides unit local diversity in the lower tail.

Evaluating the local diversity for  $g \rightarrow -\infty$  dB reduces to the value of the classic diversity. This approach allows to study how well a lower tail approximation represents the behaviour of the radio channel in the UR-relevant region.

## IV. RICIAN FADING CHANNEL REVISITED

We will consider Rician fading channels with Rician  $K$  factor and diffuse power  $P_{\text{dif}}$ , following the parametrisation in [9]. The  $K$  factor describes the ratio between a dominant deterministic component and the diffuse power of the radio channel. Hence, the mean power gain is  $(K + 1)P_{\text{dif}}$ .

To take  $M$  uncorrelated antennas at the base station into account, a complex random vector with mean  $\sqrt{KP_{\text{dif}}}[e^{j\phi_1}, e^{j\phi_2}, \dots, e^{j\phi_M}]^T$  and covariance  $P_{\text{dif}}\mathbf{I}$  is constructed:

$$\mathbf{h} \in \mathbb{C}^M \sim \mathcal{CN}\left(\sqrt{KP_{\text{dif}}}[e^{j\phi_1}, e^{j\phi_2}, \dots, e^{j\phi_M}]^T, P_{\text{dif}}\mathbf{I}\right). \quad (3)$$

The phases  $\phi_m$  represent the phase front of the deterministic component with respect to the antennas and  $\mathbf{I}$  is the  $M \times M$  identity matrix. For Rayleigh fading ( $K = 0$ ) reduces the description to a circular-symmetric complex normal random vector  $\mathbf{h} \sim \mathcal{CN}(0, P_{\text{dif}}\mathbf{I})$ .

Applying maximal ratio combining (MRC) at the receiver gives the effective channel coefficient  $\mathfrak{h}$  and related effective power gain  $\mathfrak{g}$  (on a linear scale):

$$\mathfrak{g} = |\mathfrak{h}|^2 = \mathbf{h}^H \mathbf{h} = \sum_{m=1}^M |h_m|^2. \quad (4)$$

The CDF  $F(\mathfrak{g}; P_{\text{dif}}, K, M)$  of the effective gain of this multi-antenna Rician channel is compactly given by:

$$F(\mathfrak{g}; P_{\text{dif}}, K, M) = P_M \left( KM, \frac{\mathfrak{g}}{P_{\text{dif}}} \right), \quad (5)$$

where  $P_M(\cdot)$  is the complementary Marcum Q-function [10] with definition<sup>1</sup>:

$$P_\mu(x, y) = x^{\frac{1}{2}(1-\mu)} \int_0^y t^{\frac{1}{2}(\mu-1)} e^{-t-x} I_{\mu-1} \left( 2\sqrt{xt} \right) dt. \quad (6)$$

This power gain CDF is a generalised [11] or non-central gamma distribution [12] arising from a sum over squared per-antenna channel coefficients in Eqn. (4).

The distribution relates to a  $\kappa$ - $\mu$  envelope distribution [13], where the number of independent antenna elements corresponds to  $\mu$  clusters and the  $K$  factor relates to the ratio  $\kappa$  between dominant and scattered channel components for a mean normalised to unity. The connection between a single antenna Rayleigh channel, the complementary Marcum Q-function and the effective gain CDF to arrive at a non-central gamma distribution is described in detail in the appendix A and the connection to the  $\kappa$ - $\mu$  envelope distribution follows directly from comparison of the CDFs being based on Marcum-Q functions.

The mean of the distribution is:

$$\mathcal{E} \{ \mathfrak{g} \} = M(K+1)P_{\text{dif}}, \quad (7)$$

which follows from adding  $M$  independent Rician channels with the same  $K$  factor and power in the diffuse component. Varying  $K$  factors for different antenna elements could be accounted for by using the mean  $K$  factor in the above formulation. Both the  $K$  factor and the number of antenna elements  $M$ , have the similar influence on the mean of the distribution.

Fig. 2a shows a selection of CDFs that describe the behaviour of a single antenna Rice channel. The channel gain is normalised with its mean to allow easier comparison of the small-scale fading aspects for different  $K$  factors. A stronger deterministic component leads to a dual slope behaviour, with a steeper gradient closer to the median of the distribution. Nonetheless, the gradient converges to 10 dB per decade in the lower tail, independent of the  $K$  factor. The very seldom cases occur only when the diffuse components cancel the deterministic component almost perfectly. For a  $K$  factor of 10 dB, the gradient is steepest in the region between -15 dB and 0 dB with respect to the mean. This indicates that the lower

<sup>1</sup>Note that this definition is a different variant of the implementation found in major numeric computing environments, but the reference [10] provides a Fortran implementation together with the numerical algorithm description.

TABLE I  
NORMALISED LOCAL DIVERSITY  $D/M$  EVALUATED AT  $10^{-6}$  PROBABILITY. THE DIFFERENT COLOURED REGIONS SHOW WHERE THE ASYMPTOTIC TAIL APPROXIMATION HOLDS (GREEN), UNDERESTIMATES (RED) OR OVERESTIMATES (BLUE) THE SLOPE IN THE UR-RELEVANT REGIME.

$K$ [dB]	Number of Antennas ( $M$ )							
	1	2	4	8	16	32	64	128
$-\infty$	1.00	1.00	0.99	0.92	0.80	0.65	0.50	0.38
0.0	1.00	1.00	1.00	0.97	0.87	0.72	0.57	0.43
3.0	1.00	1.00	1.07	1.13	1.03	0.86	0.67	0.51
6.0	1.00	1.07	1.48	1.56	1.38	1.12	0.86	0.64
10.0	1.09	2.66	3.07	2.77	2.25	1.74	1.31	0.96
20.0	23.39	19.02	14.68	10.99	8.08	5.86	4.22	3.02

tail approximation underestimates the channel behaviour for outage probabilities ranging from  $10^{-4}$  to 0.5.

The corresponding PDF  $f(\mathfrak{g})$  is more involved:

$$f(\mathfrak{g}; P_{\text{dif}}, K, M) = \begin{cases} \frac{1}{P_{\text{dif}}} e^{-\frac{\mathfrak{g}}{P_{\text{dif}}}} - K I_0 \left( 2\sqrt{K \frac{\mathfrak{g}}{P_{\text{dif}}}} \right) & M = 1 \\ \frac{1}{P_{\text{dif}}} \left( P_{M-1} \left( KM, \frac{\mathfrak{g}}{P_{\text{dif}}} \right) - P_M \left( KM, \frac{\mathfrak{g}}{P_{\text{dif}}} \right) \right) & M > 1 \end{cases} \quad (8)$$

where  $I_0(\cdot)$  is the zero-order modified Bessel function of the first kind. For the multi-antenna case, we can exploit the relation for derivatives of the complementary Marcum-Q function [10, Sec. 2.3].

Finally, the local diversity for arrays can be expressed based on the complementary Marcum-Q function for  $M > 2$  and explicit calculations of PDF and CDF for a single antenna:

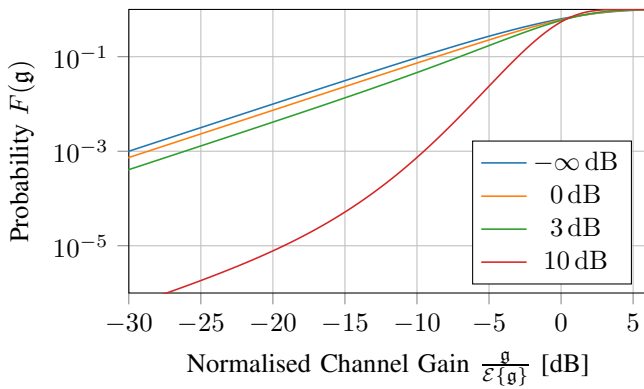
$$D(\mathfrak{g}; P_{\text{dif}}, K, M) = \frac{\mathfrak{g}}{P_{\text{dif}}} \left( \frac{P_{M-1} \left( KM, \frac{\mathfrak{g}}{P_{\text{dif}}} \right)}{P_M \left( KM, \frac{\mathfrak{g}}{P_{\text{dif}}} \right)} - 1 \right), \quad (9)$$

since the algorithm in [10] only provides solutions for  $P_\mu(\cdot)$  with  $\mu \geq 1$ .

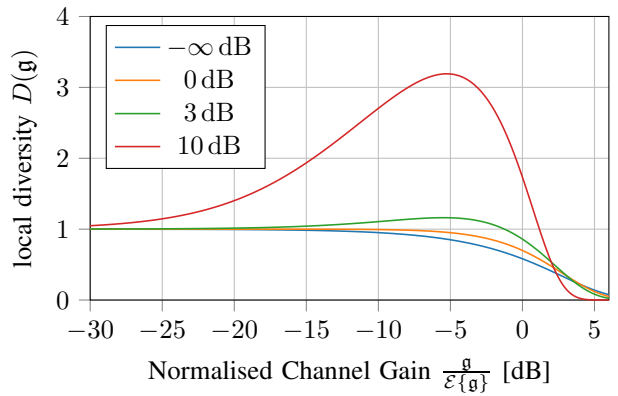
Fig. 2b presents the local diversity for a Rician single antenna channel ( $M = 1$ ) with respect to the effective channel gain. Larger  $K$  factors lead to superelevation before convergence to unity and the local diversity quantifies the increased steepness in Fig. 2a.

Fig. 3 plots the local diversity with respect to probability to interpret its behaviour in the UR-relevant regime. The superelevation is pronounced in the region from  $10^{-6}$  to 0.5 for a  $K$  factor of 10 dB. All other  $K$  factors have converged to a local diversity of unity for probabilities smaller than  $10^{-3}$ .

This behaviour changes for larger arrays and is exemplified by the normalised local diversity in Figs. 4a and 4b for a Rayleigh and Rician channel with  $K$  factor 10 dB, respectively. Table I summarises these results at a probability of  $10^{-6}$  over different  $K$  factors and number of antennas  $M$ . The normalisation is provided by dividing the local diversity with the number of antennas. Hence, once the normalised local diversity attains unity, the classic diversity of  $M$  for large SNR is achieved. The normalised local diversity can therefore be interpreted as relative error between a lower tail approximation



(a) CDFs



(b) local diversity

Fig. 2. The normalised single antenna Rician channel is displayed for different  $K$  factors. The normalisation enforces unit mean. Larger  $K$  factors give a dual slope CDF which is corresponding to the superelevation of the local diversity.

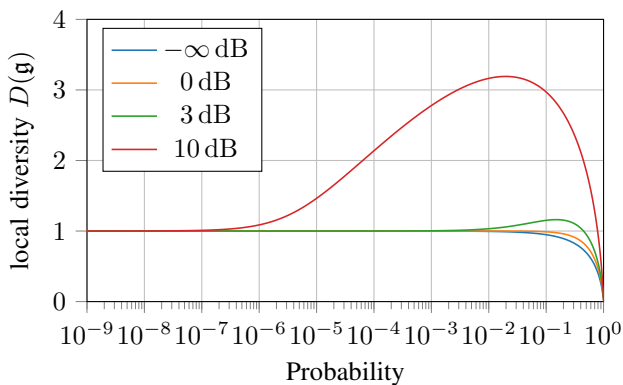


Fig. 3. The local diversity with respect to probability of a single antenna Rician channel for different  $K$  factors.

and the actual steepness of the effective gain CDF at the chosen probability.

## V. DISCUSSION

The relative error of diversity is provided in Tab. I, revealing three different connected regions. The first region (green) is covering small  $K$  factors for small systems, where the normalised local diversity is close to unity. A lower tail approximation will give reasonable results for UR-relevant statistics. The second region (blue) belongs to Rayleigh fading and smaller  $K$  factors for an increasing number of antennas. In this case, the local diversity has not yet converged to unity and a lower tail approximation will overestimate the performance accordingly. E.g. a 64 antenna element array in Rayleigh fading at a probability of  $10^{-6}$  will only provide the performance predicted by the asymptotic regime of a 32 antenna system. For large systems, only significant deterministic components will provide superelevation in the region of interest. The last region (red) belongs to large  $K$  factors, where the local diversity is larger than the diversity, e.g. an environment with a  $K$  factor of 10 dB and 4 antennas presents a local diversity of  $4 \cdot 3.07 \approx 12$

TABLE II  
ANALYTIC FADING MARGINS IN DB AT  $10^{-6}$  PROBABILITY.

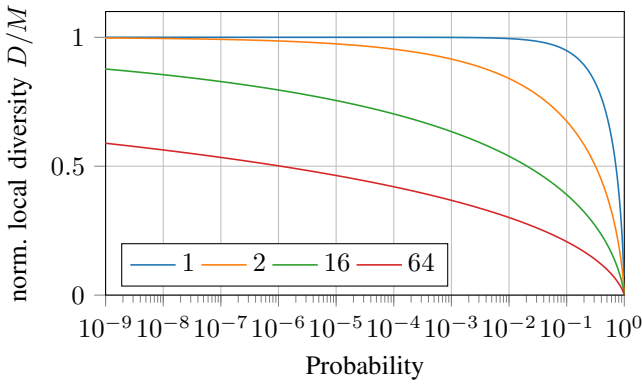
$K$ [dB]	Number of Antennas ( $M$ )							
	1	2	4	8	16	32	64	128
$-\infty$	58.4	30.7	17.1	10.2	6.5	4.3	2.9	2.0
0.0	57.6	29.7	16.0	9.3	5.7	3.7	2.5	1.7
3.0	55.3	27.3	13.9	7.8	4.9	3.2	2.1	1.5
6.0	49.2	21.3	10.2	6.0	3.8	2.5	1.7	1.2
10.0	27.2	10.4	5.9	3.7	2.5	1.7	1.2	0.8
20.0	3.5	2.3	1.6	1.1	0.8	0.5	0.4	0.3

in the superelevated probability region. The superelevation moves towards smaller probabilities for an increasing number of antennas. Overall, the deterministic component of a Rician fading environment plays a role for every  $K$  factor for large antenna systems and a growing  $K$  factor increases the local diversity.

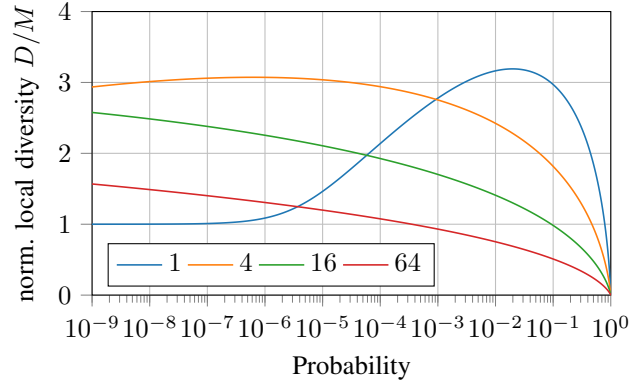
To relate the local diversity to a more tangible figure of merit, the fading margin has been evaluated for the same parameters as the normalised local diversity and the result is presented in Table II. This highlights the return on investment of extra power or antenna gain, to improve the reliability of a system. Similarly, for a fixed output power, the backoff for a rate selection algorithm can be set accordingly to achieve UR outage probabilities.

In the following the impact of array deployment strategies for URLLC applications is discussed. Every increase of the deterministic component will improve the robustness. Hence, it is worthwhile to compare a larger co-located system with a smaller  $K$  factor to smaller spatially distributed deployments. The latter system is expected to have at least one subarray in an environment with larger  $K$  factor, as is potentially closer to a user.

As an example: a co-located uncorrelated 64 antenna base station in a Rician fading environment with  $K = 0 \text{ dB} = 1$  would require a fading margin of 2.5 dB at an outage probability for  $10^{-6}$  for a mean effective gain of  $64 \cdot (1 + 1)P_{\text{diff}} =$



(a) Rayleigh Fading



(b) Rician Fading ( $K = 10$  dB)

Fig. 4. Normalised local diversity for an  $M$ -antenna array with 1, 2, 16 or 64 elements. A tail approximation would underestimate the outage behaviour of the system for larger arrays in Rayleigh fading and overestimate it in Rician fading.

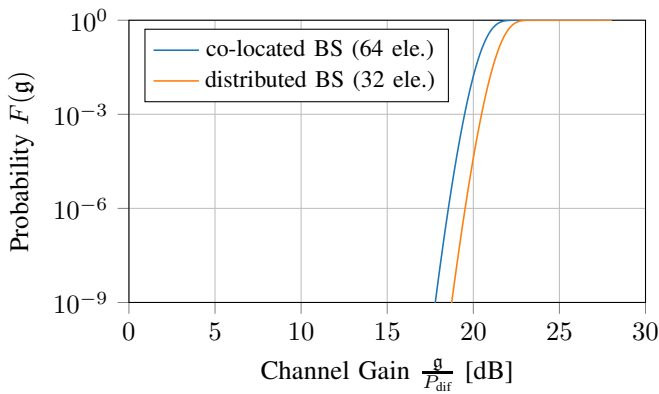


Fig. 5. CDFs of a co-located 64 antenna base station with  $K$  factor 0 dB (blue) and the closest distributed 32 antenna base station (orange) with  $K$  factor 6 dB. The stronger deterministic component of the channel in the distributed base station case compensates for the reduced number of antennas, resulting in a similar local diversity at  $10^{-6}$ , giving a slight advantage with respect to the mean of the channel gain.

$128P_{\text{dif}}$ . Placing two non-cooperating uncorrelated 32 antenna base stations instead into that environment and reducing the length of the deterministic path to a half for a user could increase the  $K$ -factor to 6 dB. The closer of those two base stations would then require a fading margin of 2.5 dB at an outage probability for  $10^{-6}$ . For this setting the mean gain would be  $32 * (4 + 1)P_{\text{dif}} = 160P_{\text{dif}}$ . Their CDFs are shown in Fig. 5, where the slope of both has not yet converged to the asymptotic behaviour of the lower tail in the UR-relevant regime. In this toy example, distributed base stations requiring the same amount of hardware would give equal fading margins and even an increased mean effective gain with respect to the co-located case. To put it short, densification of base stations can give an advantage over co-located larger installations even from an UR-relevant statistics perspective and not only for capacity improvements.

If a URLLC system has to rely only on diffuse propagation, then increasing the number of base station antennas gives diminishing returns. For fading environments with deterministic

propagation components, the number of antenna elements per base station influences where the normalised local diversity shows superelevation.

So, how can we infer the system behaviour of events that barely ever happen? Given a limited number of measurable samples from each antenna element, how could the UR-relevant statistics be analysed in real world systems? There are two basic approaches for ultra-reliable antenna arrays: The first is based on collection of antenna element observations, estimation of each distribution and careful modeling of correlation properties. Antenna elements that belong to the same large-scale fading region could be lumped into a single distribution to make more samples available. Post-processing of the resulting distributions with combination strategies like selection combining (SC) or MRC result in a CDF to be evaluated in the UR-relevant regime. In case of SC, it is not necessary to have a reliable estimate of the antenna element CDFs in that regime, but rather in the regime resulting from the  $M$ -th root of the target outage probability. This follows from the maximum order statistic for the strongest constituent, being the  $M$ -th power of the element CDF. Since MRC will give a better combined gain than SC, using a SC result allows to bound the system behaviour in the UR-relevant regime based on reliable estimates of the element CDFs.

The second approach implements a specific combination strategy, evaluating the UR-relevant statistics directly. This includes intrinsically antenna correlation, avoiding the necessity of explicit characterisation. Unfortunately, this strategy requires prohibitively many observations. Even for the first approach a lot of samples are necessary, but the antenna element observations do not need to be observed in the UR-relevant regime directly, since this regime only matters for the effective gain is of channel. Furthermore, the correlation is expected to depend to a lesser extent on the combined channel stationarity, allowing them to be studied in more detail with help of all antenna element observations.

## VI. CONCLUSION

Acquisition of UR-relevant channel statistics is difficult to achieve in practical situations, because the number of required observations is tremendous. Ultimately, the stationarity of the radio channel restricts the duration of measurement collection. The approach of using the asymptotic lower tail behaviour can be used for small arrays up to four antennas in low  $K$  factor Rician fading. Systems that provide large diversity, require consideration of the local diversity in the UR-relevant regime. There, the asymptotic behaviour applies to very low probabilities only.

The local diversity can be used to analyse distributions at UR-relevant outage probabilities. Normalisation with the number of antenna elements in an array gives a relative deviation from the classic diversity and opens up for performance evaluation, where measurements of correlated antenna systems can be compared to an uncorrelated optimum.

For fast and numerically stable calculations, the distribution and local diversity of the effective gain of an uncorrelated antenna array can be formulated on the basis of the complementary Marcum-Q function. Evaluation of the fading margin and distribution mean reinforces that a dense deployment of smaller base stations with the potential for increased deterministic radio channels is preferable over very large co-located systems, not only improving system capacity but also robustness.

## APPENDIX

### A. CDF of the Effective Power Gain

The *non-central gamma distribution* has PDF  $w_\rho(x; \alpha, \mu)$  for index  $\rho$ , scale  $\alpha$ , and non-centrality  $\mu$  [12, (1.47')] for  $x \geq 0$ :

$$w_\rho(x; \alpha, \mu) = \frac{1}{\alpha} e^{-\frac{x}{\alpha} - \mu} \left( \frac{x}{\alpha \mu} \right)^{\frac{1}{2}(\rho-1)} I_{\rho-1} \left( 2\sqrt{\frac{\mu x}{\alpha}} \right). \quad (10)$$

The corresponding CDF  $W_\rho(x; \alpha, \mu)$  can be directly related to the definition of the complementary Marcum Q-function in Eqn. (6) by substitution of  $t = \frac{x'}{\alpha}$  in the integral relation between CDF and PDF:

$$W_\rho(x; \alpha, \mu) = \int_0^x w_\rho(x'; \alpha, \mu) dx' = P_\rho(\mu, \frac{x}{\alpha}). \quad (11)$$

The gain PDF  $f_{\mathfrak{G}}(\mathfrak{g}; P_{\text{dif}}, M = 1, K)$  of a single antenna Rician channel is readily available by using the Rician envelope PDF from [9, (5.3.7)] applying the transformation to the power PDF [9, (5.2.1)] and replacing the power term of the deterministic component [9, (5.3.8)], resulting in:

$$\begin{aligned} f(\mathfrak{g}; P_{\text{dif}}, K, M = 1) \\ &= \frac{1}{P_{\text{dif}}} \exp\left(-\frac{\mathfrak{g}}{P_{\text{dif}}} - K\right) I_0\left(2\sqrt{K\frac{\mathfrak{g}}{P_{\text{dif}}}}\right) \\ &= w_1(\mathfrak{g}; P_{\text{dif}}, K). \end{aligned} \quad (12)$$

This PDF is a special case of the non-central gamma distribution PDF in Eqn. (10) for index one, scale  $P_{\text{dif}}$  and non-centrality  $K$ .

For  $M$  independent single antenna Rician channels with potentially differing  $K$  factors  $K_m \forall m \in [1, \dots, M]$  the additive property of non-central gamma distributions can be used to get the PDF of the effective channel gain. The addition property allows to represent the sum of independent random variables with the same scale, potentially varying index and non-centrality as non-central gamma distribution [12, (1.51)]. The generalisation of Eqn. (12) for an  $M$  antenna array follows a non-central gamma distribution of index  $M$  and non-centrality  $\sum_{m=1}^M K_m$ :

$$f(\mathfrak{g}; P_{\text{dif}}, K, M) = w_M\left(\mathfrak{g}; P_{\text{dif}}, \sum_{m=1}^M K_m\right). \quad (13)$$

Using Eqn. (11) gives the CDF of the effective channel gain based on the inverse Marcum Q-function:

$$F(\mathfrak{g}; P_{\text{dif}}, M, K) = P_M\left(\sum_{m=1}^M K_m, \frac{\mathfrak{g}}{P_{\text{dif}}}\right). \quad (14)$$

## REFERENCES

- [1] H. Ji, S. Park, J. Yeo, Y. Kim, J. Lee, and B. Shim, "Ultra-Reliable and Low-Latency Communications in 5G Downlink: Physical Layer Aspects," *IEEE Wireless Communications*, vol. 25, no. 3, pp. 124–130, Jun. 2018. DOI: 10.1109/MWC.2018.1700294.
- [2] P. C. F. Eggers, M. Angelichinoski, and P. Popovski, "Wireless Channel Modeling Perspectives for Ultra-Reliable Communications," *IEEE Transactions on Wireless Communications*, vol. 18, no. 4, pp. 2229–2243, Apr. 2019. DOI: 10.1109/TWC.2019.2901788. arXiv: 1705.01725.
- [3] J. Abraham and T. Ekman. (2021). "Fading Margins for Large-Scale Antenna Systems." accepted at 2021 IEEE International Conference on Communications (ICC): Wireless Communications Symposium. arXiv: 2102.09903.
- [4] H. Yan, A. Ashikhmin, and H. Yang, *Can Massive MIMO Support URLLC?* to appear in the 2021 IEEE 93rd Vehicular Technology Conference (VTC2021-Spring), 2021. arXiv: 2102.09156.
- [5] M. Angelichinoski, K. F. Trillingsgaard, and P. Popovski, "A Statistical Learning Approach to Ultra-Reliable Low Latency Communication," *IEEE Transactions on Communications*, vol. 67, no. 7, pp. 5153–5166, Jul. 2019. DOI: 10.1109/TCOMM.2019.2907241.
- [6] D. Tse and P. Viswanath, *Fundamentals of Wireless Communication*, 1st ed. Cambridge University Press, May 26, 2005. DOI: 10.1017/CBO9780511807213.
- [7] A. Dvoretzky, J. Kiefer, and J. Wolfowitz, "Asymptotic Minimax Character of the Sample Distribution Function and of the Classical Multinomial Estimator," *The Annals of Mathematical Statistics*, vol. 27, no. 3, pp. 642–669, Sep. 1956. DOI: 10.1214/aoms/1177728174.
- [8] P. Massart, "The Tight Constant in the Dvoretzky-Kiefer-Wolfowitz Inequality," *The Annals of Probability*, vol. 18, no. 3, pp. 1269–1283, Jul. 1990. DOI: 10.1214/aop/1176990746.
- [9] G. D. Durgin, *Space-Time Wireless Channels*, ser. Prentice Hall communications engineering and emerging technologies series. Upper Saddle River, NJ: Prentice Hall PTR, 2003.
- [10] A. Gil, J. Segura, and N. M. Temme, "Algorithm 939: Computation of the Marcum Q-Function," *ACM Transactions on Mathematical Software*, vol. 40, no. 3, pp. 1–21, Apr. 2014. DOI: 10.1145/2591004.
- [11] E. W. Stacy, "A generalization of the gamma distribution," *The Annals of Mathematical Statistics*, vol. 33, no. 3, pp. 1187–1192, Sep. 1962. DOI: 10.1214/aoms/1177704481.
- [12] H. Ruben, "Non-central chi-square and gamma revisited," *Communications in Statistics*, vol. 3, no. 7, pp. 607–633, Jan. 1974. DOI: 10.1080/03610927408827163.
- [13] M. Yacoub, "The  $\kappa$ - $\mu$  distribution and the  $\eta$ - $\mu$  distribution," *IEEE Antennas and Propagation Magazine*, vol. 49, no. 1, pp. 68–81, Feb. 2007. DOI: 10.1109/MAP.2007.370983.